

The Extensional and Failure Properties of Polymer Melts

T. TAKAKI* and D. C. BOGUE, *Department of Chemical and Metallurgical
Engineering, University of Tennessee, Knoxville, Tennessee 37916*

Synopsis

The extensional and failure properties of polystyrene melts were studied by pulling sample rods in a special "weight dropping" extensometer. This apparatus allows pulling to long final lengths and at relatively high rates; except for the highest rates, the experiment is one of constant applied force. Various commercial (broad molecular weight distribution) and special (narrow molecular weight distribution) samples were studied at various temperatures and applied forces. The striking result was that the former (BMWD) samples stretched reasonably uniformly and displayed what has been described as "viscoelastic failure"; the latter (NMWD) samples necked in the final stages and showed what might be called "viscous" failure. In the case of the BMWD material, the stress-time behavior was analyzed theoretically by independently determining the parameters in a nonlinear constitutive equation from GPC and rheogoniometer (shear) data. The theoretical tensile stresses compared quite well with the experimental values. An interesting result came from comparing the complete viscoelastic theory with a viscous (Trouton viscosity) asymptote. These two theoretical curves closely approximated the experimental data until just short of the failure point; at this incipient point, the stresses from the complete theory grew to very large values compared with the viscous stresses. That is, the material could not relax fast enough to allow steady stresses to develop, and the sample failed shortly thereafter.

INTRODUCTION

For many years, rheological research has centered on shear flows and existing rheological theory has largely been developed from such experiments. Recently, however, extensional flow has received increasing attention, both as a basic problem in rheology and as it relates to industrial applications such as fiber spinning. Under the heading of basic studies, the research has mostly been organized around fluid concepts, involving the variables of elongation rate and elongational viscosity. In a later section, generalized strain tensors will be presented and these call for stating a relationship between time and the length of the extending rod, that is, $L(t)$. An extension rate $\dot{\epsilon}$ can then be defined by

$$\dot{\epsilon} = \frac{1}{L(t)} \frac{dL(t)}{dt}. \quad (1)$$

* Present address: Ube Industries, Inc., Hirakata Plastics Laboratory, Hirakata Osaka-fu, Japan.

If $\dot{\epsilon}$ is constant (true elongation rate), this leads to

$$L(t) = L_0 \exp(\dot{\epsilon}t) \quad (2)$$

where L_0 is the original length of the sample. A true elongational viscosity $\bar{\eta}$ can then be defined by

$$\bar{\eta} = \frac{S_{11}}{\dot{\epsilon}} \quad (3)$$

where S_{11} is the total tensile stress. At low values of $\dot{\epsilon}$, it is well known that $\bar{\eta}$ is equal to three times the shear viscosity (the Trouton viscosity¹). In many experiments, one does not achieve a constant elongation rate, and in such cases one sometimes defines an apparent elongational viscosity by using eq. (3) with instantaneous values of S_{11} and $\dot{\epsilon}$.

In 1965, Ballman² made the first measurements on a polymer melt (polystyrene) under conditions of constant $\dot{\epsilon}$. Recently, there have been a number of experiments of this type, notably those of Vinogradov³ and Meissner.⁴ More complicated experiments, which do not involve constant $\dot{\epsilon}$, involve entry flows⁵ and "melt spinning" type of flows.⁵⁻⁹

On the theoretical side elongation experiments have been analyzed using integral theories of viscoelasticity. Chang and Lodge¹⁰ used a linear model to analyze Meissner's constant $\dot{\epsilon}$ experiments, and our group at the University of Tennessee has used a nonlinear model to analyze both the melt-spinning type of experiment and the constant-force (weight dropping) type of experiment.⁷ In general, one concludes that the theory works well in cases where the initial state of the sample is well characterized. Other work with a nonlinear model has been reported by Middleman.¹¹

Failure properties of polymer melts have not been so widely studied, although there is, of course, a considerable literature on solid-like (cross-linked) materials.^{12,13} The most extensive work on melts is that of Kamei and Onogi¹⁴ and Onogi, Matsumoto, and Kamei¹⁵ at Kyoto University, who worked with well-characterized polystyrene samples. The striking result from their work is the great similarity of the stress at break versus $\dot{\epsilon}$ curves to the relaxation spectra curves. In the failure curves, the Kyoto group identifies distinct regimes which they label as "brittle," "viscoelastic," "transition," and "viscous" failure, the latter being characterized by necking and flow prior to failure. On the theoretical side, an analysis due to Chang and Lodge,¹⁶ to be discussed later, is directly related to the necking-to-failure mechanism.

EXPERIMENTAL

The present work deals with an (essentially) constant force experiment, performed in a "weight dropping" apparatus; that is, a falling weight extends a molten sample in a heated chamber. This is not an easy experiment to do but it has the advantage of allowing long extensions at relatively high rates. In previous work, as reported by Chen et al.,⁷ results from this apparatus (using polyethylene samples) were compared with

results from the melt-spinning type of apparatus; the results were quite different, even though both experiments are, to a first approximation, experiments of constant force. In the present work, the objective was to carry out detailed elongational studies with well-characterized samples (polystyrenes of known molecular weight distributions), with special emphasis on failure properties.

Materials

Three materials were studied, two commercial (broad molecular weight distribution = BMWD) samples and one special (narrow molecular weight distribution = NMWD) sample. The properties of these materials are summarized in Table I.

A few qualitative remarks will be made about the Piccolastic material, but mostly the following has to do with the Shell (BMWD) and Pressure Chemical (NMWD) samples. The molecular weight distributions were determined on a Waters GPC, as described elsewhere.¹⁷ Independent rheological characterization (in shear) was carried out on a Weissenberg rheogoniometer for the Shell and Piccolastic materials, of which the Shell data is displayed in Figures 1 and 2. For the sharp distribution sample,

TABLE I
Materials Used in the Present Experiments

Polystyrene	Manufacturer's value		From GPC (University of Tennessee)		
	M_n	M_w	M_n	M_w	M_w/M_n
Shell TC3-30 ^a	61.2×10^3	283×10^3	59.0×10^3	312×10^3	5.30
Piccolastic D-150 ^b	5	—	4.20	74.5	17.8
Batch No. 3b ^c	355	392	329	408	1.24

^a Manufactured by Shell Chemical Company.

^b Manufactured by Pennsylvania Industrial Chemical Corporation.

^c Manufactured by Pressure Chemical Corporation.

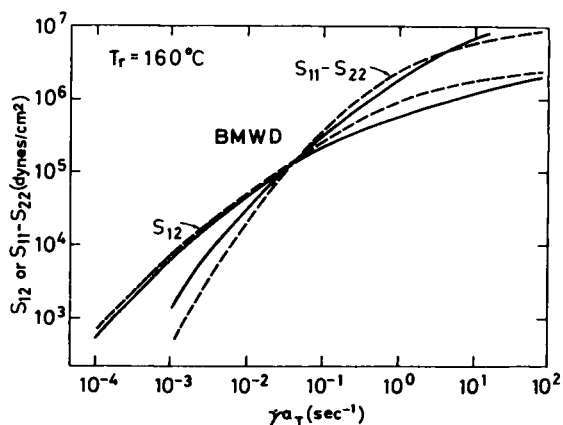


Fig. 1. Steady shear properties (reduced to 160°C).

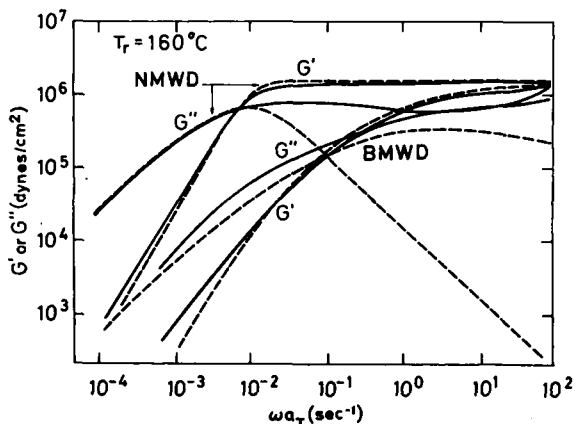


Fig. 2. Dynamic shear properties (reduced to 160°C). NMWD curves are taken from Onogi et al.¹⁸

G' and G'' data are available from Onogi et al.,¹⁸ and these are shown in Figure 2. The Shell sample data were obtained at 160°, 170°, 180°, and 200°C and reduced to a reference temperature (T_r) of 160°C by means of a time-temperature superposition shift factor a_T as given by the following relationship:

$$\log a_T(T) = 694.8 \left(\frac{1}{T - 46.7} - \frac{1}{T_r - 46.7} \right) \quad (4)$$

where the temperature T is given in °C. Onogi et al.,¹⁸ used a similar shift factor for NMWD materials. In Figures 1 and 2, the solid lines are the experimental curves and the dotted lines are the theoretical curves, to be discussed later.

Procedure

The basic apparatus was developed by Hagler,⁷ but was modified in the present work to allow in situ melting of the sample (see Fig. 3). The experimental sample rods (about 0.61 cm in diameter and 3–6 cm in length) were prepared from the original pellets or powder by molding in a glass tube, after which the ends were melted slightly and the sample made into a spool-piece shape. The ends were then inserted into special clamps and the entire clamp/sample assembly lowered into the circulating oil bath at the top of the apparatus. After melting (about 10 min or so), the oil was very quickly drained from the sample chamber (in about 5 sec), after which the trap door was released, allowing the falling weight to pull the molten sample down through the heated chamber (80 cm long). The length-time data were obtained in two ways: (1) using a marker train and photoelectric cell system, and (2) using a linear differential transducer system. The core of the latter was 5.6 in. long, and this apparatus could thus be used for the shorter lengths. Various recorders were used to record the length-time history. The total mass was taken as the sum of the falling weight, the clamps and associated wires, and the sample, but

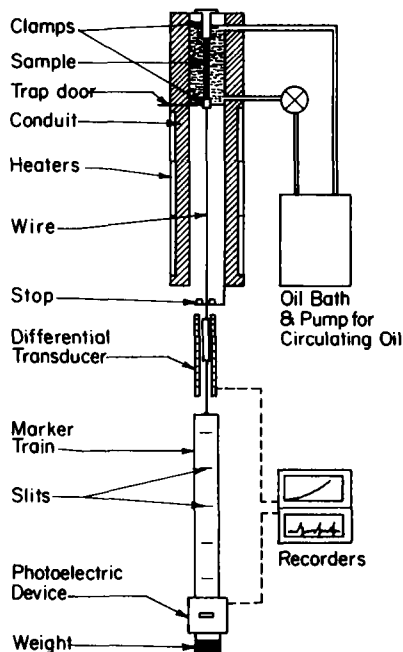


Fig. 3. Schematic diagram of extensometer.

the mass of the sample was small compared with the total (about 8% in the worst case) and was neglected. The radius of the extending sample was calculated by assuming uniform radius over the length, which was approximately realized in the case of the Shell sample but not so in the final flow stages of the Pressure Chemical sample (which necked severely).

Several weights and six temperatures from 150° to 200°C were used, depending on the sample. A time-temperature superposition was carried out on the data, the shift factor in elongation being about the same as that in shear at small times but differing significantly at higher times. The data reported here will all be at the reference temperature of 160°C, with the exception of one set of data for the NMWD material. 160°C data are not available for this material.

Experimental problems were slumping of the samples during melting and pulling of the sample from the clamps. These were serious difficulties in the case of two lower molecular weight NMWD samples (not reported here) and at higher temperatures.

Presentation of Experimental Results

The interesting difference between the two materials is that the NMWD samples flowed slowly and uniformly until just before failure, at which point they necked and broke in the neck. The BMWD samples, on the other hand, extended out reasonably uniformly up to the break point. This tendency of NMWD samples to fail seems to have general validity and has been observed, for example, in the processing of rubber¹⁸ and in the shear behavior of a large number of materials.²⁰

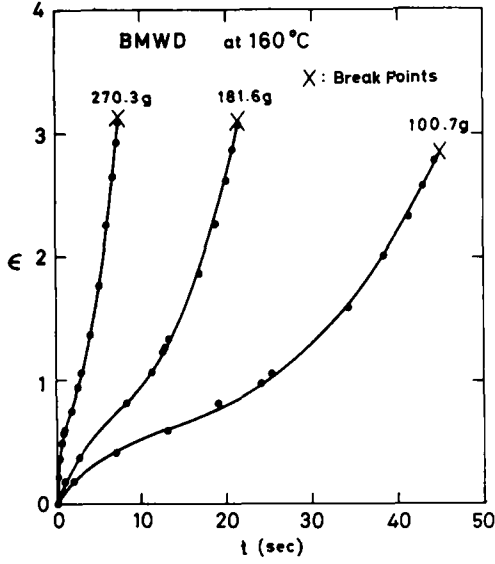


Fig. 4. Typical strain-time curves for BMWD material. Symbols are the data; lines are curve-fitted results from eq. (11).

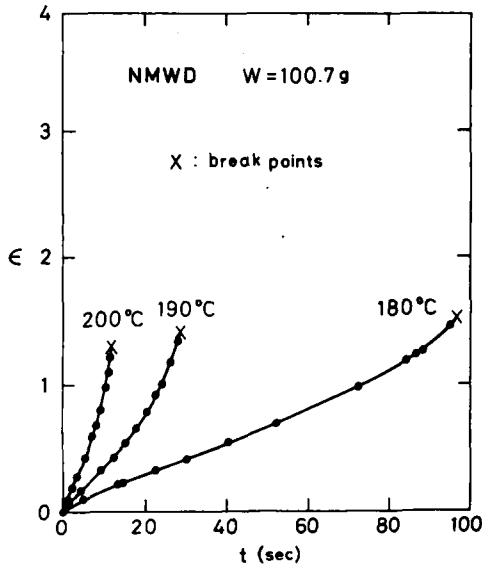


Fig. 5. Typical strain-time curves for NMWD material.

The length-time data are presented almost directly as measured in Figures 4 and 5, these being typical curves for the two materials. The strain ϵ there is defined by

$$\epsilon = \ln \left(\frac{L(t)}{L_0} \right) \tag{5}$$

One notes that the strains at break for the NMWD samples are considerably lower than for the BMWD samples (the former samples necked at break). In Takaki's thesis,¹⁷ a comparison of the failure conditions with those of Onogi et al.,^{14,15} was made at comparable molecular weights; the results were that the BMWD sample falls in the "viscoelastic" failure regime and the sharp distribution sample, in the "viscous" regime. This is consistent with the necking (or non-necking) behavior which we observed and which led Onogi et al. to assign these descriptions to the regimes involved. The Piccolastic sample, not shown here, flowed out into quite long filaments and did not break within the experimental length, apparently due to the "lubrication effect" of a small molecular weight component.

VISCOELASTIC ANALYSIS

BMWD Materials

In the cases where the sample could be pulled out reasonably uniformly (the BMWD Shell samples), the rheological response was analyzed with viscoelastic theory. In linear viscoelasticity, it is possible to use either the relaxation spectrum (the Maxwell model) or the retardation spectrum (the Voigt model); the latter is useful in experiments with stress as the applied variable and, for simpler deformations, leads to an elastic parameter called the steady-state compliance.²¹ In generalized nonlinear theory, however, there is no counterpart to the Voigt model. The relative importance of the viscoelastic, viscous, and elastic responses can be understood, however, by calculating certain asymptotes, as will be done later.

The model used was that of Bogue,²² as modified by Bogue and White.²³ This model has been tested in both shear²⁴ and elongation.⁷ In terms of discrete spectra, it can be stated as follows:

$$S_{ij} = -p\delta_{ij} + \int_{-\infty}^t \sum_p G_p \frac{e^{-(t-t')/\tau_p^*}}{\tau_p^*} c_{ij}^{-1}(t,t') dt' \quad (6)$$

where S_{ij} is the total stress, p is the isotropic pressure, and the G_p are the elastic moduli. Also,

$$\tau_p^* = \frac{\tau_p}{1 + A\tau_p K} = \text{effective time constants}$$

$$K = \frac{\int_{t'}^t \Pi_d^{1/2} dt''}{t - t'} = \text{average deformation rate}$$

Π_d = second invariant of the deformation rate tensor

$$c_{ij}^{-1} = \frac{\partial x_i}{\partial X_k} \frac{\partial x_j}{\partial X_l} \delta_{kl} = \text{Finger strain tensor}$$

where τ_p are the material time constants, t is the present time, t' and t'' are arbitrary past times (the variables of integration), and A is an adjustable constant.

In order to evaluate the various moduli and to make some connection with molecular theory, a modification of eq. (6), that is, a molecular weight model adapted from Bogue et al.,²⁵ was used:

$$S_{ij} = -p\delta_{ij} + G^* \int_{-\infty}^t \sum_{p=1}^N \sum_{q=1}^N w_p w_q \frac{e^{-(t-t')/\tau_{pq}^*}}{\tau_{pq}^*} c_{ij}^{-1}(t,t') dt' \quad (7)$$

where w_p is the weight fraction of molecular weight species M_p , G^* is the elastic modulus of the entanglement (rubbery) region, and N is the number of molecular weight species.

This is a quadratic blending law and is valid, or reasonably so, in the so-called "entanglement" regime of high molecular weight (in the case of polystyrene, above a molecular weight of about 30,000). As discussed by Masuda,²⁶ this model works well in the extreme of one molecular weight predominating, but not so well in intermediate regimes. Despite these difficulties, it was used here in order to obtain some qualitative understanding of the role of molecular weight on the extensional behavior. To adjust for the difficulties in the model, an adjustable parameter (M_{avg}) was introduced in the definition of the time constants:

$$\tau_{pq}^* = \frac{\sqrt{\tau_p \tau_q}}{1 + A \sqrt{\tau_p \tau_q} \bar{K}} \quad (8)$$

where

$$\frac{\tau_p}{\tau_{\text{ref}}} = \left(\frac{M_p}{M_{\text{ref}}} \right)^2 \left(\frac{M_{\text{avg}}}{M_{\text{ref}}} \right)^{1.5}.$$

M_{avg} is presumed to lie somewhere between M_n and M_w (in the original model, it is taken equal to M_w); τ_{ref} and M_{ref} are, respectively, a reference time constant and a reference molecular weight. Using the data of Onogi et al.,¹⁸ these were taken as $\tau_{\text{ref}} = 500$ sec at $M_{\text{ref}} = 580,000$ (at 160°C).

In order to evaluate the moduli in eq. (7) shear stress, normal stress, and dynamic (G' and G'') data were taken on the Weissenberg rheogoniometer. A five-component molecular weight distribution ($N = 5$) was used (see Fig. 6); because of the quadratic mixing law, this gives, in effect, a 25-element relaxation spectrum, which was felt to be a good approximation to a continuous spectrum. The parameters A and M_{avg} were adjusted to give reasonable fits to the rheogoniometer data. The equations used to fit the shear data are omitted here.²²

The theoretical curves are shown by the dotted lines in Figures 1 and 2. While there are some discrepancies in the fit, it was felt that the model reflected the essential features of the shear data, except for G'' in the case of the sharp distribution sample. The parameters used are summarized as follows: $G^* = 1.8 \times 10^6$ dynes/cm², $A = 0.5$, $M_{\text{avg}} = 47,180$, $M_p = 5,800$ ($w_p = 0.06$), 32,500 (0.27), 200,000 (0.46), 800,000 (0.19), and 3,200,000 (0.02).

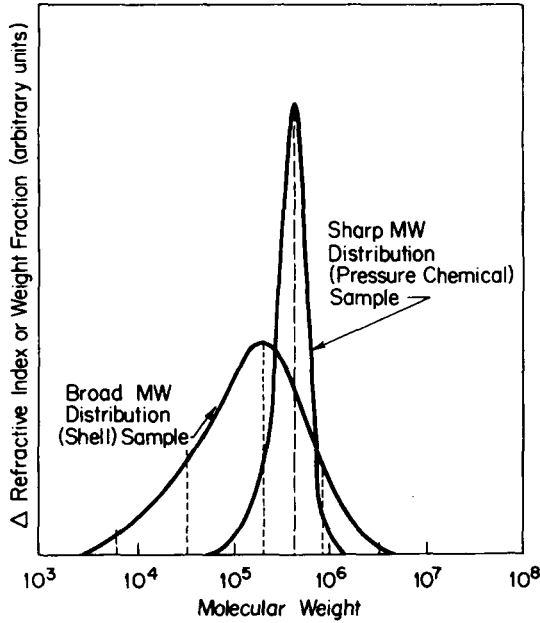


Fig. 6. Molecular weight distributions. The dotted lines show the discrete distribution used in the theoretical model.

In the case of the elongational (weight-dropping) flow, the tensile stress $S_{11}(t)$ was calculated as follows:

$$S_{11}(t) = G^* \int_0^{\ln s_{\max}} \sum_{p=1}^5 \sum_{q=1}^5 w_p w_q \frac{e^{-s \tau_{pq}^*}}{\tau_{pq}^*} \left[\left(\frac{L(t)}{L(t')} \right)^2 - \left(\frac{L(t)}{L(t')} \right)^{-1} \right] s ds \ln s$$

(full viscoelastic theory) (9)

where $s = t - t'$, $L(t)$ = length of sample at time t , $L(t')$ = length of sample at time t' ,

$$\tau_{pq}^* = \frac{\sqrt{\tau_p \tau_q}}{1 + A \sqrt{\tau_p \tau_q} \bar{K}}$$

and

$$\bar{K} = \frac{\ln(L(t)/L(t'))}{s}$$

The length functions were obtained by curve-fitting equations of the following form to the experimental length-time data:

$$\ln(L(t)/L_0) = 0 \quad \text{for } t < 0 \quad (10)$$

$$\ln(L(t)/L_0) = at^{1/2} + bt + ct^{3/2} + dt^2 \quad \text{for } t > 0 \quad (11)$$

Similarly for t' . The lines shown in Figure 4 are calculated from eq. (11). The integration of eq. (9) was carried out numerically using 100 trapezoidal

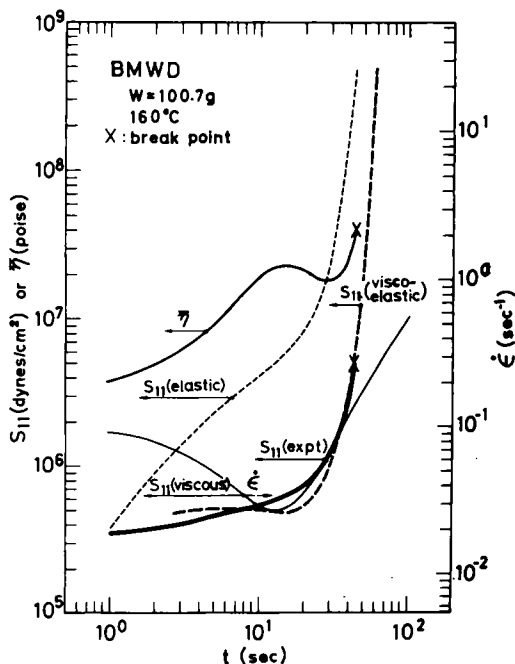


Fig. 7. Experimental and theoretical stresses, apparent elongational viscosity and elongation rate (BMWD material, small weight): expt = experimental data; viscoelastic = full viscoelastic theory; viscous = Trouton viscosity asymptote; elastic = elastic asymptote.

increments in $\ln s$ and taking a value for s_{\max} equal to 100 times the relaxation time for the highest molecular weight present.

For comparison, two asymptotes were also calculated as follows:

$$S_{11}(t) = G^* \left[\left(\frac{L(t)}{L_0} \right)^2 - \left(\frac{L(t)}{L_0} \right)^{-1} \right] \quad (\text{elastic asymptote}) \quad (12)$$

$$S_{11}(t) = 3G^* \sum_{p=1}^5 \sum_{q=1}^5 w_p w_q \sqrt{\tau_p \tau_q} \dot{\epsilon} \quad (\text{viscous or Trouton asymptote}) \quad (13)$$

$$\text{where } \dot{\epsilon} = \frac{1}{L(t)} \frac{dL(t)}{dt}.$$

The first is rubber elasticity theory,²⁷ and the second uses the Trouton viscosity noted previously.

These various theoretical stresses can then be compared with the experimental stress data, which were processed by the following equation:

$$S_{11}(t) = \frac{m \left[g_L - \frac{d^2 L}{dt^2} \right]}{\pi R^2} \quad (\text{experimental}) \quad (14)$$

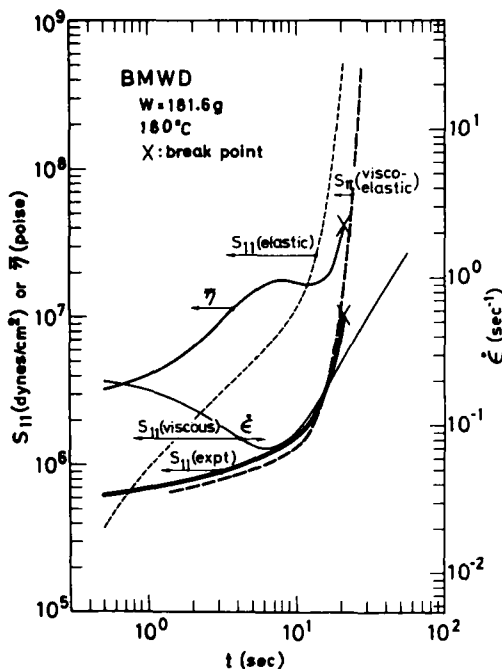


Fig. 8. Experimental and theoretical stresses, apparent elongational viscosity and elongation rate (BMW material, intermediate weight): expt = experimental data; viscoelastic = full viscoelastic theory; viscous = Trouton viscosity asymptote; elastic = elastic asymptote.

where m is the mass of the falling weight and associated clamps, etc., g_L is the acceleration due to gravity, and R is the instantaneous radius. In the cases discussed here, the acceleration term d^2L/dt^2 was small. The stresses are shown in Figures 7, 8, 9, together with an apparent elongational viscosity calculated directly from the experimental data, using point values of S_{11} and $\dot{\epsilon}$.

The general observation is that the full viscoelastic theory gives a good fit to the data. This is an encouraging result because all of the rheological parameters have been established a priori (from shear data).

The comparison of the full theory (or the data) with the elastic and viscous asymptotes is instructive. Qualitative understanding can be gotten by studying the data of Meissner,⁴ who did experiments at constant $\dot{\epsilon}$, starting from rest. Using the materials and the rheology of the present work, a plot like that of Meissner's is shown in Figure 10. This is a theoretical prediction of a transient start-up at constant $\dot{\epsilon}$. That is,

$$L(t) = L_0 \exp[\dot{\epsilon}t] \quad \text{for } t > 0.$$

At short times the stresses have not had time to build to their steady flow viscous values. At small $\dot{\epsilon}$ a steady state is achieved, corresponding to the Trouton viscosity asymptote. At high $\dot{\epsilon}$, however, no steady state is

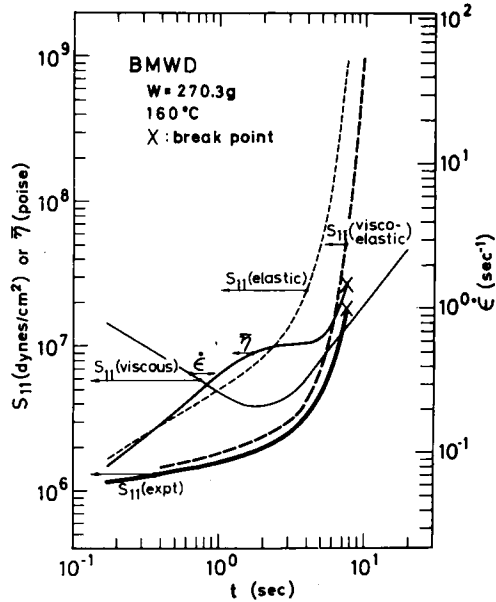


Fig. 9. Experimental and theoretical stresses, apparent elongational viscosity, and elongation rate (BMWD material, large weight): expt = experimental data; viscoelastic = full viscoelastic theory; viscous = Trouton viscosity asymptote; elastic = elastic asymptote.

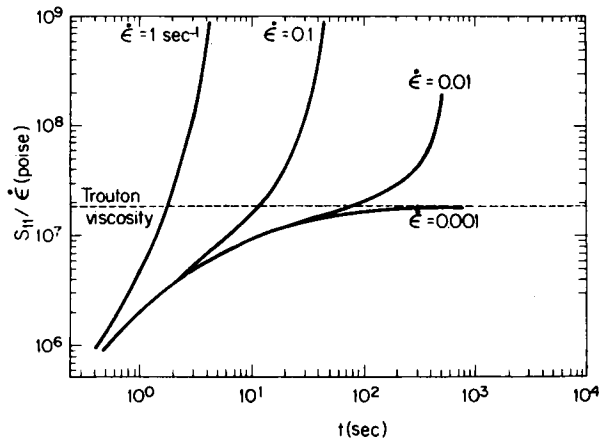


Fig. 10. Hypothetical stress development after starting at constant elongation rate (theoretical simulation of BMWD material).

achieved, and the stresses go to infinity. All of these effects may be seen qualitatively in the present experiments (Figs. 7, 8, and 9). At low times, the data (and the viscoelastic theory) fall below the viscous asymptote. At a point just before failure, the viscous and viscoelastic lines approach each other closely. Soon however, the viscoelastic stress begins to grow

very rapidly, and shortly thereafter the sample fails. In molecular terms, one would say the extending molecules cannot relax fast enough to flow. A somewhat similar physical picture, based on the concept of a highly elastic state of almost zero fluidity, is presented by Vinogradov et al.²⁰ for experiments in shear.

NMWD Materials

The NMWD sample cannot be so easily handled since it necked in the final stages, making the assumption of uniform diameter not valid near the failure point. However, to verify that the theory would give values of the correct magnitude, the above analysis was repeated, using a single molecular weight species as shown in Figure 6, and the results are shown in Figure 11. Even allowing for uncertainties near the failure point, the agreement is satisfactory.

Qualitative understanding can be obtained by considering the analysis of Chang and Lodge¹⁶ who studied the extension of two connected rods of slightly different diameters. In the extreme of a Newtonian fluid, the thin part gets rapidly thinner; in the case of a viscoelastic material, the thin part and the thick part both get thinner, but the ratio of the cross-sectional areas tends to a constant. One would suppose that the first case would correspond to $\dot{\epsilon} \ll \tau_{\max}^{-1}$, where τ_{\max} is some appropriately defined

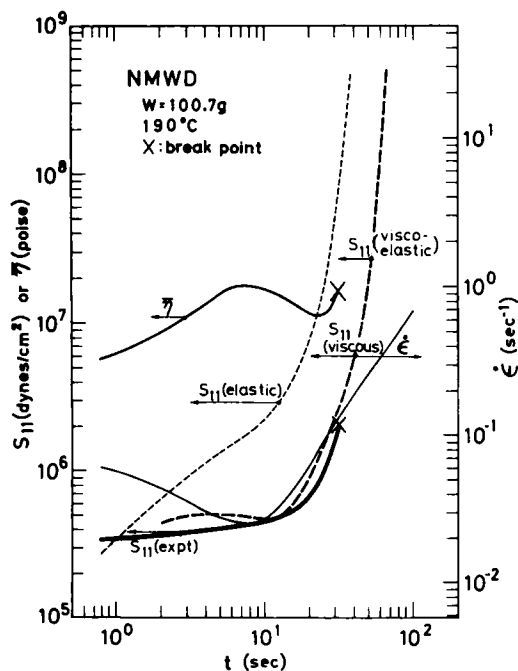


Fig. 11. Experimental and theoretical stresses, apparent elongational viscosity, and elongation rate (NMWD material): expt = experimental data; viscoelastic = full viscoelastic theory; viscous = Trouton viscosity asymptote; elastic = elastic asymptote.

maximum relaxation time. For a NMWD material, one can select a characteristic and unique relaxation time from the data of Onogi et al.¹⁸ [see the equation for τ_p after eq. (8)]. Using this equation and adjusting to 190°C by the NMWD equivalent of eq. (4), one obtains a characteristic relaxation time of about 3.4 sec. Thus, we would conclude that if $\dot{\epsilon} \ll 1/3.4 = 0.3 \text{ sec}^{-1}$, the failure would be "Newtonian" in the Chang-Lodge sense. The experimental $\dot{\epsilon}$'s leading to necking failure are of the order of 0.1 sec^{-1} at 190°C (Fig. 11); thus, it is not unreasonable to associate the failure noted experimentally and the Chang-Lodge Newtonian flow failure.

CONCLUDING REMARKS

We feel that the essential features of the flow and failure of polymer melts can be explained within the framework of present-day viscoelastic theory. If necking does not occur, the sample extends out reasonably uniformly, and viscoelastic theory provides a very good prediction of the stresses. Failure is associated with the point where the complete (viscoelastic) stress diverges considerably from the viscous stress. Of course, viscoelastic theory does not provide a criterion for failure as such; but if one presumes that some kind of network failure is involved, one could propose a criterion based on the difference between the full viscoelastic stress and the viscous stress (i.e., on the elastic stress or strain).

The authors acknowledge with thanks the support of the National Science Foundation (under Grant GK-18897) and the Polymer Consortium Industrial Group at the University of Tennessee for their support of this work.

References

1. F. T. Trouton, *Proc. Royal Soc.*, **A77**, 427 (1906).
2. R. L. Ballman, *Rheol. Acta* **4**, 137 (1965).
3. G. V. Vinogradov, V. D. Fikhman, and B. V. Radushkevich, *Rheol. Acta*, **11**, 286 (1972); (with A. Ya. Malkin) *J. Polym. Sci. A-2*, **8**, 657 (1970); *ibid.*, **8**, 1 (1970).
4. J. Meissner, *Rheol. Acta*, **8**, 78 (1969); *ibid.*, **10**, 230 (1971); *Trans. Soc. Rheol.*, **13**, 123 (1969); *ibid.*, **16**, 405 (1972).
5. F. N. Cogswell, *Rheol. Acta*, **8**, 187 (1969); *Trans. Soc. Rheol.*, **16**, 383 (1972); *Poly. Eng. Sci.*, **12**, 64 (1972).
6. D. Acierno, J. N. Dalton, J. M. Rodriguez, and J. L. White, *Appl. Polym. Sci.*, **15**, 2395 (1971).
7. I-J. Chen, G. E. Hagler, L. E. Abbott, D. C. Bogue, and J. L. White, *Trans. Soc. Rheol.*, **16**, 473 (1972).
8. G. M. Fehn, *J. Poly. Sci. A-1*, **6**, 247 (1968).
9. J. A. Spearot and A. B. Metzner, *Trans. Soc. Rheol.*, **16**, 495 (1972).
10. H. Chang and A. S. Lodge, *Rheol. Acta*, **11**, 127 (1972).
11. S. Middleman, *Trans. Soc. Rheol.*, **13**, 123 (1969).
12. R. F. Landel and R. F. Fedors, in *Fracture Processes in Polymeric Solids: Phenomena and Theory*, B. Rosen, Ed., Interscience, New York, 1964.
13. T. L. Smith, in *Rheology*, Vol. 5, F. R. Eirich, Ed., Academic Press, New York, 1969.
14. E. Kamei and S. Onogi, Proceedings of the 20th Meeting of Rheology, Fukui, Japan, October 1972 (in Japanese).
15. S. Onogi, T. Matsumoto, and E. Kamei, *Polymer J.*, **3**, 531 (1972).

16. H. Chang and A. S. Lodge, *Rheol. Acta*, **10**, 448 (1971).
17. T. Takaki, M.S. Thesis, Chemical Engineering, University of Tennessee, Knoxville, Tennessee, 1973.
18. S. Onogi, et al., *Macromolecules*, **3**, Part I, 109 (1970); S. Onogi, T. Masuda, and K. Kitagawa, *ibid.*, Part II, 116 (1970).
19. J. L. White, *Rubber Chem. Technol.*, **52**, 257 (1969).
20. G. V. Vinogradov, A. Ya. Malkin, Yu. G. Yanovskii, E. K. Borisenkova, B. V. Yarlykov, and G. V. Berezhnaya, *J. Polym. Sci. A-2*, **10**, 1061 (1972).
21. J. D. Ferry, *Viscoelastic Properties of Polymers*, 2nd ed., Wiley, New York, 1970.
22. D. C. Bogue, *Ind. Eng. Chem., Fundam.*, **5**, 253 (1966).
23. D. C. Bogue and J. L. White, *Engineering Analysis of Non-Newtonian Fluids*, NATO Agradograph 144, 1970.
24. I-J Chen and D. C. Bogue, *Trans. Soc. Rheol.*, **16**, 59 (1972).
25. D. C. Bogue, T. Masuda, Y. Einaga, and S. Onogi, *Polym. J.*, **1**, 563 (1970).
26. T. Masuda, Ph.D. Dissertation, Polymer Chemistry, Kyoto University, Kyoto, 1973.
27. T. R. G. Treloar, *The Physics of Rubber Elasticity*, 2nd ed., Oxford University Press, London, 1958.

Received June 10, 1974

Revised July 30, 1974